

Upconversion luminescence and decay kinetics in a diode-pumped nanocrystalline Nd³⁺:YVO₄ random laser

Renato Juliani Ribamar Vieira,¹ Laércio Gomes,¹ José Roberto Martinelli,²
and Niklaus Ursus Wetter^{1,*}

¹Centro de Lasers e Aplicações, Instituto de Pesquisas Energéticas e Nucleares IPEN-CNEN/SP, Av. Lineu Prestes 2242, 005508-000 São Paulo, Brazil

²Centro de Ciência e Tecnologia de Materiais, IPEN-CNEN/SP, Av. Lineu Prestes 2242, 005508-000 São Paulo, Brazil

*nuwetter@ipen.br

Abstract: Random lasing in nanocrystalline Nd³⁺:YVO₄ powder is demonstrated. A method that analyzes the decay kinetics after long-pulse excitation is used to determine the laser characteristics. This method permits to measure the fractional contribution of spontaneous and stimulated emission as well as upconversion as a function of the pump intensity. We observed that maximum linewidth narrowing is achieved when the stimulated emission reaches 50% of fractional contribution in the backscattering cone.

©2012 Optical Society of America

OCIS codes: (140.3480) Lasers, diode-pumped; (290.1990) Diffusion; (290.4210) Multiple scattering.

References and links

1. V. S. Letokhov, "Generation of ultrashort light pulses in laser with nonlinear absorbent," *Sov. Phys. JETP* **26**, 835–840 (1968).
2. C. Gouedard, D. Husson, C. Sauteret, F. Auzel, and A. Migus, "Generation of spatially incoherent short pulses in laser-pumped neodymium stoichiometric crystals and powders," *J. Opt. Soc. Am. B* **10**(12), 2358–2363 (1993).
3. B. Li and S. C. Rand, "Continuous-wave amplification and light storage in optically and electrically pumped random laser media," *J. Opt. Soc. Am. B* **24**(4), 799–807 (2007).
4. D. S. Wiersma, "The physics and applications of random lasers," *Nat. Phys.* **4**(5), 359–367 (2008).
5. Y. Feng, S. Huang, G. Qin, M. Musha, and K. I. Ueda, "Random microchip laser," *Opt. Express* **13**(1), 121–126 (2005).
6. Y. Feng, J.-F. Bisson, J. Lu, S. Huang, K. Takaichi, A. Shirakawa, M. Musha, and K.-I. Ueda, "Thermal effects in quasi-continuous-wave Nd³⁺:Y₃Al₅O₁₂ nanocrystalline-powder random laser," *Appl. Phys. Lett.* **84**(7), 1040–1042 (2004).
7. M. A. Noginov, I. Fowlkes, G. Zhu, and J. Novak, "Neodymium random lasers operating in different pumping regimes," *J. Mod. Opt.* **51**(16-18), 2543–2553 (2004).
8. K. L. van der Molen, A. P. Mosk, and A. Lagendijk, "Relaxation oscillations in long-pulsed random lasers," *Phys. Rev. A* **80**(5), 055803 (2009).
9. M. A. Noginov, N. E. Noginova, H. J. Caulfield, P. Venkateswarlu, T. Thompson, M. Mahdi, and V. Ostroumov, "Short-pulsed stimulated emission in the powders of NdAl₃(BO₃)₄, NdSc₃(BO₃)₄, and Nd:Sr₂(PO₄)₃F laser crystals," *J. Opt. Soc. Am. B* **13**(9), 2024–2033 (1996).
10. J. Azkargorta, M. Bettinelli, I. Iparraguirre, S. Garcia-Revilla, R. Balda, and J. Fernández, "Random lasing in Nd:LuVO₄ crystal powder," *Opt. Express* **19**(20), 19591–19599 (2011).
11. M. Bahoura, K. J. Morris, G. Zhu, and M. A. Noginov, "Dependence of the neodymium random laser threshold on the diameter of the pumped spot," *IEEE J. Quantum Electron.* **41**(5), 677–685 (2005).
12. B. A. van Tiggelen, D. S. Wiersma, and A. Lagendijk, "Self-consistent Theory for the Enhancement Factor in Coherent Backscattering," *Europhys. Lett.* **30**(1), 1–6 (1995).
13. B. Michel, "Mie Calc-freely configurable, on-line program for light scattering calculations (Mie theory)," <http://www.lightscattering.de/MieCalc/eindex.html>.
14. D. S. Wiersma and A. Lagendijk, "Light diffusion with gain and random lasers," *Phys. Rev. E Stat. Phys. Plasmas Fluids Relat. Interdiscip. Topics* **54**(4), 4256–4265 (1996).
15. D. S. Wiersma, P. Bartolini, A. Lagendijk, and R. Righini, "Localization of light in a disordered medium," *Nature* **390**(6661), 671–673 (1997).

16. A. Sennaroglu, "Influence of neodymium concentration on the strength of thermal effects in continuous-wave diode-pumped Nd:YVO₄ laser at 1064 nm," *Opt. Quantum Electron.* **32**(12), 1307–1317 (2000).
 17. C. Jacinto, S. L. Oliveira, T. Catundab, A. A. Andrade, J. D. Myers, and M. J. Myers, "Upconversion effect on fluorescence quantum efficiency and heat generation in Nd³⁺-doped materials," *Opt. Express* **13**(6), 2040–2046 (2005).
 18. X. D. Li, X. Yu, J. Gao, F. Chen, J. H. Yu, and D. Y. Chen, "Upconversion spectra of Nd:GdVO₄ crystal under CW 808 nm diode-laser pumping," *Laser Phys. Lett.* **6**(2), 125–128 (2009).
 19. M. Pollnau, D. R. Gamelin, S. R. Lüthi, H. U. Güdel, and M. P. Hehlen, "Power dependence of upconversion luminescence in lanthanide and transition-metal-ion system," *Phys. Rev. B* **61**(5), 3337–3346 (2000).
 20. M. Inokuti and F. Hirayama, "Influence of energy transfer by the exchange mechanism on donor luminescence," *J. Chem. Phys.* **43**(6), 1978–1989 (1965).
-

1. Introduction

The possibility of generating stimulated emission in disordered media (random lasers) was predicted in the 1960s by Lethokov [1], and experimentally demonstrated in the 1990s [2]. These highly scattering gain media present several interesting features that cannot be achieved with conventional lasers, such as simultaneous emission of several different wavelengths and emission at new extremely low gain lines [3,4]. Additionally, the microscopic dimensions and the lack of polished surfaces are particularly interesting for integrating this laser into optic devices.

Only few reports exist on diode pumped random lasers [5,6]. This technique, which is especially suited for high gain materials such as neodymium (Nd) doped materials requires generally that the pump pulse duration is of the order of the spontaneous decay time. As opposed to the usual short pulse pumping technique, this quasi-continuous pumping regime presents qualitative changes in the emission kinetics of the random lasers' stimulated emission [7]. The lasers' characteristic relaxation oscillations are normally used to demonstrate in the time domain that the system undergoes laser action [7]. However, the observation of these spikes not only depends on the pump power and the detector type, but also on the kind of nanopowder and the pump duration [6].

Mosk *et al* [8] presented a detailed theoretical and experimental work on the relaxation oscillations in long-pumped random lasers for a liquid dye containing scatters, concluding that in order to observe relaxations oscillations the linewidth of the laser cavity must be smaller than of the laser medium, a condition which is fulfilled for a dye emission, where the emission linewidth is much larger than the characteristic escape rate of photons from the random laser volume which acts as the cavity, but not necessarily will occur for a ceramic sample like described in Ref [7]. Noginov *et al* show that under strong pumping density the upconversion influences the decay kinetics from a Nd:Al₃(BO₃)₄ sample [9]. Azkargorta *et al* demonstrated linewidth narrowing in Nd:LuVO₄ using short (10 ns) pump pulses and achieved good agreement of observed threshold behavior and multiple pulsing behavior with a rate-equation model [10]. However, to our knowledge, no explanations have been performed of the effects of upconversion in the interesting regime of long pump pulses.

In this work we demonstrate lasing action in Nd:YVO₄ nanopowder under quasi-continuous diode laser excitation, by analyzing the ⁴F_{3/2}→⁴I_{11/2} transition. A method to determine quantitatively the upconversion rate and the fraction of stimulated to spontaneous emission in the samples backscattering cone as a function of pump power is presented.

2. Characterization of the experimental set-up

The nanopowder was obtained by grinding a 1.33 mol% Nd³⁺:YVO₄ laser crystal. The concentration was determined by the EDX (energy-dispersive x-ray spectroscopy) technique. The powder morphology was determined using the Scanning electron microscopy - SEM (Cambridge Instruments, Model 360) and the distribution of particles sizes determined using the laser diffraction technique (CILAS – 825 nm) as shown in Fig. 1.

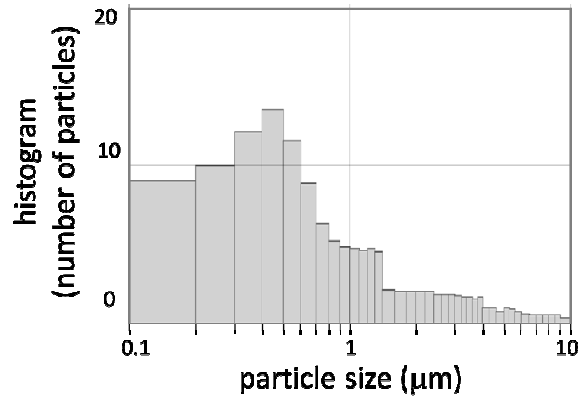


Fig. 1. Distribution of powder particles versus the diameter from the Nd:YVO₄ nanopowder sample, obtained by the laser diffraction technique (range: 0.1 to 10μm).

The mean diameter of the nanoparticles was 390 nm (range: 0.1 to 10 μm). A sample (33 mg) with flat surfaces and disk-like dimensions of 5 mm diameter was compressed to a thickness of 0.4 (±0.5) mm (Fig. 2), corresponding to a fill factor of approximately 98%. The disk was pumped by a square pump pulse from a quasi-continuous (QCW), fast-axis-collimated, 110 W laser diode bar, operating at 809 nm with 3 Hz repetition rate, 100 μs pulse width and 1 μs pulse decay time.

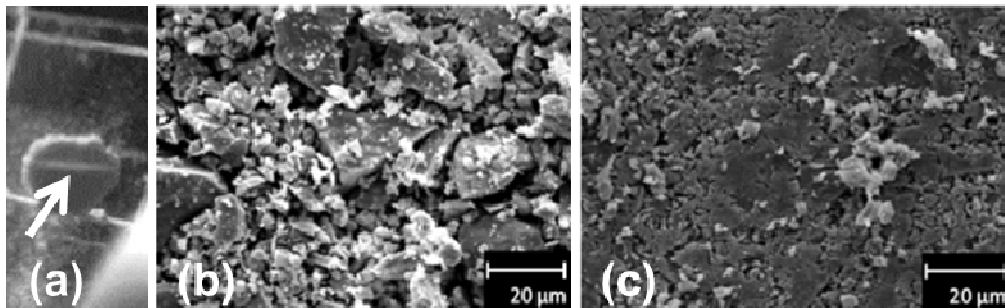


Fig. 2. (a) Disk-like sample confined by microscope slides. The line at the center of the disk (arrow) is due to visible emission from the upconversion process. (b) SEM image from the extremity of the sample. (c) SEM image from the center of the sample.

We choose a QCW laser diode as pump source, because the wavelength can be tuned to the Nd³⁺ absorption peak and pulse duration can match Nd³⁺:YVO₄ lifetime well. Therefore, enough gain can be introduced by relatively low peak pump power in QCW operation.

In Fig. 3, the experimental setup is shown. Two cylindrical divergent lenses with $f = -13$ mm and $f = -25$ mm were used for a modal conformation of the pump beam ($M_x^2=2000$ and $M_y^2=3$), such that by inserting a 20 mm spherical lens at 26 mm from the sample, a near square shaped focus of the excitation beam could be achieved at the samples surface with total area of 4.5 mm² (Fig. 4(a)).

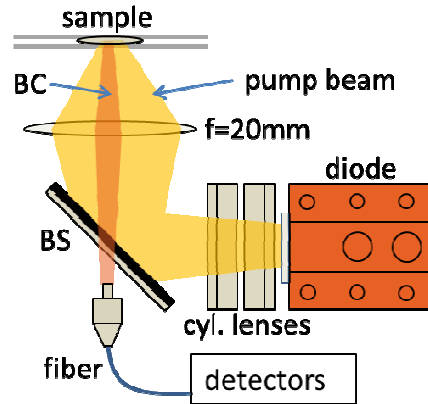


Fig. 3. Experimental setup: The 809 nm diode beam is first shaped by two cylindrical lenses with focal lengths of -13 mm and -25 mm, respectively, and then focused on the sample with a spherical $f = 20$ mm lens. The backscattering cone (BC) was separated from the pump excitation by a beam splitter (BS) and captured by fiber coupled detectors.

The pump beam size was made as small as possible in order to achieve a low threshold for laser action [11]. With the focusing lens at a distance of 35 mm, a very high intensity asymmetric beam profile was achieved as shown in Fig. 4(c) (measured with a NEWPORT CCD, model LBP-4).

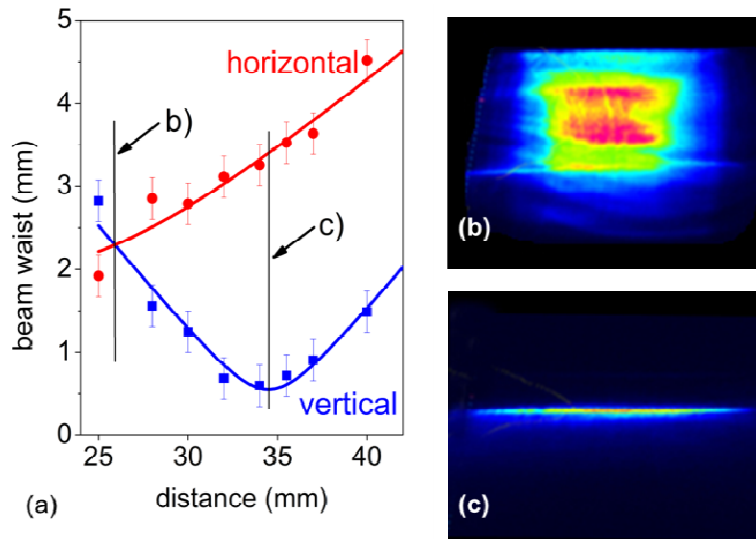


Fig. 4. (a) Beam waist measured in horizontal and vertical direction at the sample position as a function of distance from the focusing lens. (b) Beam profile observed with focusing lens at 26 mm and (c) at 35 mm.

The samples backscattered luminescence at 1064 nm was separated from the pump excitation at 808 nm by a dichroic beam splitter and analyzed using a spectrometer (Ocean Optics, Model HR2000 – resolution: 0.11 nm) and a fast oscilloscope (Lecroy, resolution 1 ns) as shown in Fig. 3. Time resolution was limited by the Germanium photo detector with 1 μ s rise time.

With this particular sample, stimulated emission was only observed at the border of the sample (within 0.5 mm of the border). Shown in Fig. 2(b) is the morphology of the extremity of the disk where laser results were observed. No laser typical emission was obtained at the

center (Fig. 2(c)). After we had already finished the present study, we fabricated another sample and achieved laser emission and linewidth narrowing at the center of the pellet. We did not investigate the exact cause for this difference, except that the second sample was less compacted (not quantified). The results presented below are from the first pellet. We used this sample because it is important for our analysis presented below to measure the backscattered light as a function of pump power in the absence of stimulated emission for all pump intensities, which could be only achieved when pumping at the center of the first sample.

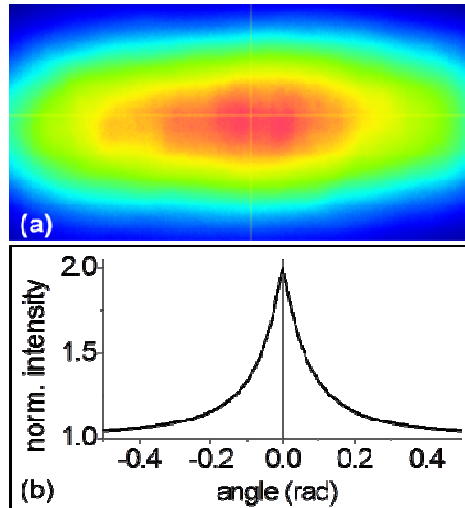


Fig. 5. (a) Backscattered cone of 1064 nm emission, obtained using a CCD digital camera. (b) Simulation of the coherent backscattered emission from this sample.

Figure 5(a) is an image of the backscattering cone taken behind the beam splitter with the focusing lens at 35 mm distance using a line filter for 1064 nm (not shown in Fig. 3). As can be observed, the backscattering cone roughly accompanies the astigmatism of the pump beam shown in Fig. 4(c). Maximum signal strength at 1064 nm at the position of the fiber connector was received within an area with typical dimensions of approximately 1 mm in height and 2 mm in width as shown in Fig. 5(a).

A disadvantage of the strong divergence and astigmatism of the pump diodes' beam is that it hampers greatly the measurement of the width of the backscattering cone, which is an important measurement in order to determine the mean free path and eventual Anderson localization. We therefore calculated the mean-free path of light in the sample by simulation, instead of measuring the width of the coherent backscattering cone, using the self-avoiding multiple scattering approximation (SAMS) [12]. For a scattering cross section of $0.16263 \mu\text{m}^2$ (determined by using the application program from reference [13]), the coherent backscatter cone, or weak localization of light, has the shape simulated in Fig. 5(b). The transport mean-free path (l_t), the average distance a wave travels before its direction of propagation is randomized, was calculated to $1.199 \mu\text{m}$ at 1064 nm. The product of $l_t k$ is 10.46, where k is the wave vector in the medium. This result describes a strong scattering medium with gain, but no Anderson localization of light, for which $l_t k < 1$ [14,15].

The result of the simulation also indicates a possible answer to the observed absence of laser emission in the center of the sample: Clearly visible in Fig. 2(c) is the much higher degree of compaction at the center when compared with the border (Fig. 2(b)). The stronger compaction results in a smaller mean free path. If the mean free path in the center of the sample is much smaller than at the border and $l_t k$ becomes close to one, the result is trapping of light (Anderson location) and laser signal intensity would be too weak to be detected at the fiber port because too few scattering centers are involved.

3. Results

At low pump intensity (2.7 W/mm^2) several fluorescent emissions ${}^4\text{G}_{7/2} \rightarrow {}^4\text{I}_{9/2}$, ${}^4\text{G}_{7/2} \rightarrow {}^4\text{I}_{11/2}$, ${}^4\text{F}_{3/2} \rightarrow {}^4\text{I}_{9/2}$, and ${}^4\text{F}_{3/2} \rightarrow {}^4\text{I}_{11/2}$ were visible from Nd^{3+} transitions.

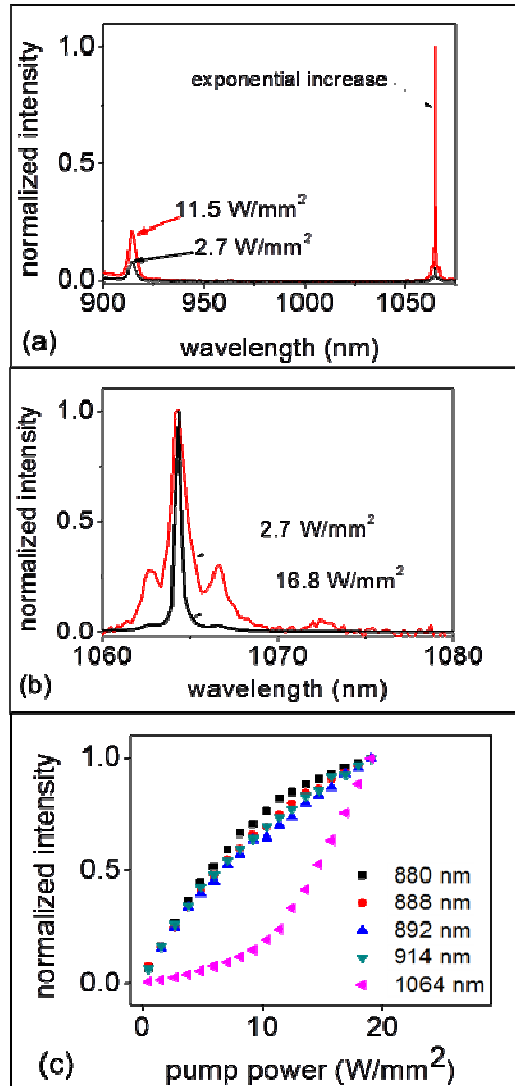


Fig. 6. (a) Emission spectra as a function of pump intensity. (b) Linewidth narrowing of the ${}^4\text{F}_{3/2} \rightarrow {}^4\text{I}_{11/2}$ emission. (c) Normalized emission intensity from optically excited $\text{Nd}^{3+}:\text{YVO}_4$ nanopowder at five wavelengths versus the incident laser power. Only the 1064 nm emission has an exponential increase.

Increasing the pump power gradually, a threshold pump intensity was observed, at which a sharp emission line at the ${}^4\text{F}_{3/2} \rightarrow {}^4\text{I}_{11/2}$ transition (1064 nm) appears, whose spectral width decreased as a function of pump power, from 1.30 nm to 0.48 nm (Fig. 6(a) and Fig. 6(b)). At low pump intensity (2.7 W/mm^2) the ${}^4\text{F}_{3/2} \rightarrow {}^4\text{I}_{9/2}$ (914 nm) transition is stronger whereas for 11.5 W/mm^2 the 1064 nm transition is strongest. Figure 6(c) shows the exponential growth for this transition (1064 nm), demonstrating that stimulated emission has been obtained. The other fluorescent emissions suffered spectral quenching.

By switching off the pump laser in less than $1\mu\text{s}$ the pulse decay features of the laser emission at 1064 nm and its spectral composition having spontaneous and stimulated emission (narrowed) contributions were analyzed. The IR-pulse decay as a function of pump power was fitted with a double exponential function. One for the spontaneous decay (τ_2) and another for the stimulated decay (τ_1). Being A the amplitude of stimulated decay and B the amplitude of the spontaneous decay, the two decay components were measured using the following Eq.:

$$I(t) = Ae^{(-t/\tau_1)} + Be^{(-t/\tau_2)} \quad (1)$$

At low pump power of 2.7 W/mm^2 of peak diode pump intensity the stimulated lifetime τ_1 was $16\ \mu\text{s}$ and the spontaneous decay time τ_2 of the transition was $62\ \mu\text{s}$ (Fig. 7(a)). At higher pump powers both lifetimes decreased as shown in Fig. 7(b) and the amplitude of stimulated emission A , increased.

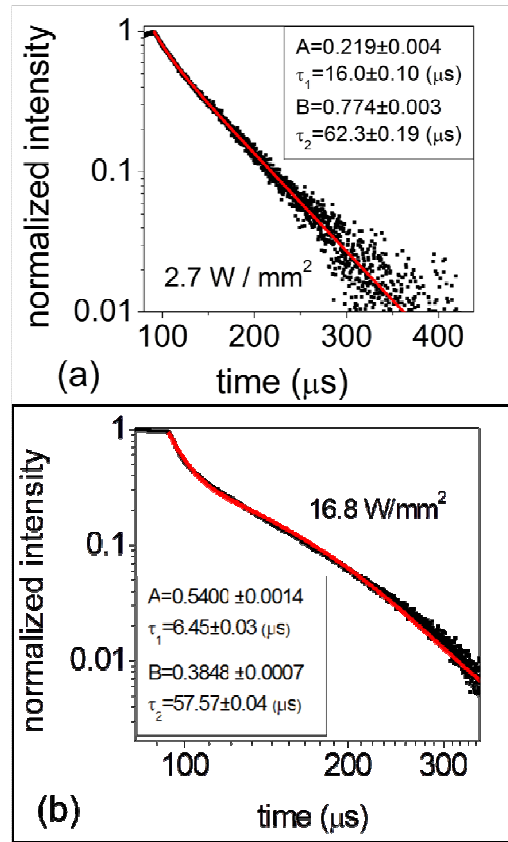


Fig. 7. (a) Laser pulse decay and fit with one exponential for a pump intensity of 2.7 W/mm^2 .
 (b) Laser pulse decay and fit with two exponentials for a pump intensity of 16.8 W/mm^2

A very interesting result of the double exponential fit in Fig. 7 is that it allows determining the fractional contribution of both components produced in the random laser, the spontaneous and the stimulated decay respectively, as a function of the pump intensity. The fraction of stimulated emission as a function of pump power, $A/(A+B)$, is shown in Fig. 8. The contribution of the stimulated emission increases with pump power. A stimulated emission fraction of 50% is achieved for a pump intensity of 15 W/mm^2 , the same pump intensity at which maximum narrowing of the emission linewidth is observed.

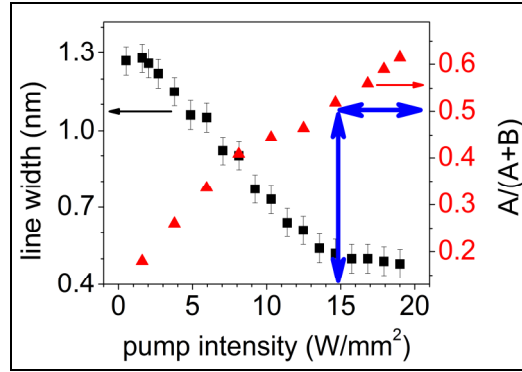


Fig. 8. Linewidth narrowing and fraction of stimulated emission at 1064 nm versus the pump power. The double arrows show that at a pump intensity of 15 W/mm² maximum linewidth narrowing is achieved and at the same time 50% of stimulated emission is detected.

From this analysis we can see that the gradual linewidth narrowing observed in our random laser as a function of pump power is due to a slow increase of the fraction of stimulated emission in the backscattering cone whilst spontaneous emission continues present up to the highest pump powers.

Although both spontaneous decay times in Fig. 7 are similar in duration, they are lower than the intrinsic decay time of 73 μ s for the ${}^4F_{3/2} \rightarrow {}^4I_{11/2}$ transition in Nd:YVO₄ doped with 1.33 mol% of neodymium given in reference [16]. In order to confirm this value before looking for other causes of this discrepancy we made a conventional luminescence spectroscopy experiment and measured the mean lifetime for the ${}^4F_{3/2}$ level as a function of pump pulse energy. By pumping a polished bulk sample of Nd:YVO₄, taken from the same location of the crystal boule from which the material of the pellet was obtained, with 10 Hz repetition rate and 4 ns pulse width from an OPO (Quantel) tuned to the pump wavelength of 808 nm, we obtained the lifetime constant of the ${}^4F_{3/2}$ excited state, shown in Fig. 9(a), when pumping with pulse energies ranging from 4.36 mJ to 15.21 mJ. Adjusting the results obtained with a third order polynomial fit, it is possible to determine a intrinsic decay time for the sample of 70.8 μ s (as expected for a sample with Nd = 1.33 mol%) in agreement with the literature [16].

We therefore suspected that the shorter decay time of the ${}^4F_{3/2}$ level is due to energy-transfer up-conversion (ETU) that lowers the intrinsic decay time. During ETU an ion is promoted to a higher-lying energy level, decaying then by fast multi-phonon relaxation back to the ${}^4F_{3/2}$ level generating thereby heat or decaying by emitting higher energy photons [17]. In both cases, the spontaneous decay time gets shortened.

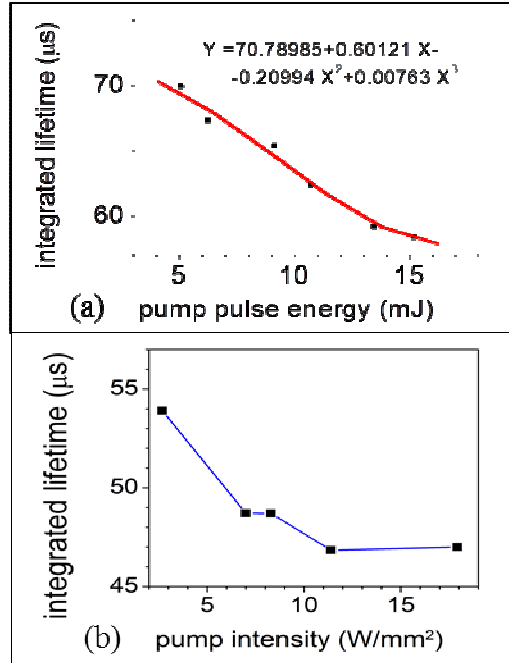


Fig. 9. (a) Determination of the radiative lifetime of the ${}^4F_{3/2} \rightarrow {}^4I_{11/2}$ transition for a Nd:YVO₄ bulk with 3 mm thickness. Fitting curve made with a third order polynomial. (b) Integrated lifetime at the center of the compressed pellet.

As already pointed out, the center of this sample showed a different morphology and was not laser active, at least not with pump intensities of up to 20 W/mm². By pumping the center of our sample we are able to make a different analysis excluding the stimulated fraction of light in the backscattering cone. We observed for higher pump energies a non-exponential decay from the ${}^4F_{3/2} \rightarrow {}^4I_{11/2}$ transition, shown in Fig. 10(a). Additionally, we observed fluorescent emissions from ${}^4G_{7/2} \rightarrow {}^4I_{15/2}$ (590 nm) and ${}^4G_{7/2} \rightarrow {}^4I_{9/2}$ (530 nm) transitions, as shown in Fig. 10(b), that are due to the (${}^4F_{3/2}, {}^4F_{3/2}$):(${}^4G_{7/2}, {}^4I_{11/2}$) up-conversion transition. These peaks can be compared to similar results obtained in Nd:GdVO₄ under diode pumping [18]. This energy transfer up-conversion (ETU) mechanism causes an additional decay rate resulting in non-exponential fluorescence decay of the ${}^4F_{3/2}$ excited level [19]. Only in the absence of stimulated emission the ETU parameters can be evaluated unambiguously and consistently as shown in Fig. 10(a) because they are retrieved from the same part of the fluorescent decay curve as stimulated emission. We used the Inokuti-Hirayama model to fit this decay because the depopulation of the upper laser level (${}^4F_{3/2}$) is due to the interionic interaction between acceptor and donor excited Nd³⁺ ions [20]:

$$I(t) = B e^{\left(\frac{-t}{\tau_i}\right)} e^{(-\gamma\sqrt{t})} \quad (2)$$

where B is the signal amplitude, τ_i the constant intrinsic lifetime of the transition, as expected from Nd³⁺ = 1.33 mol%, and γ (s^{-1/2}) the energy transfer parameter in the presence of ETU and cross-relaxation. The best fitting parameters for the (${}^4F_{3/2}$) decay exhibited in Fig. 10(a) were $B = 1$, $\gamma = 92.3$ s^{-1/2} and $\tau_i = 93.9$ μs.

The effective decay time is obtained using the relation:

$$\tau_{\text{int}} = \frac{1}{B} \int_0^{\infty} I(t) dt \quad (3)$$

The measured values of the integrated decay time τ_{int} , are shown in Fig. 9(b). The extrapolation of this curve onto the y-axis at zero pump intensity corresponds to the intrinsic decay time τ_i , at the center of the pellet and is approximately 55 μs . We note that this extrapolated intrinsic decay time at the center of the pellet is less than of the bulk (Fig. 9(a)).

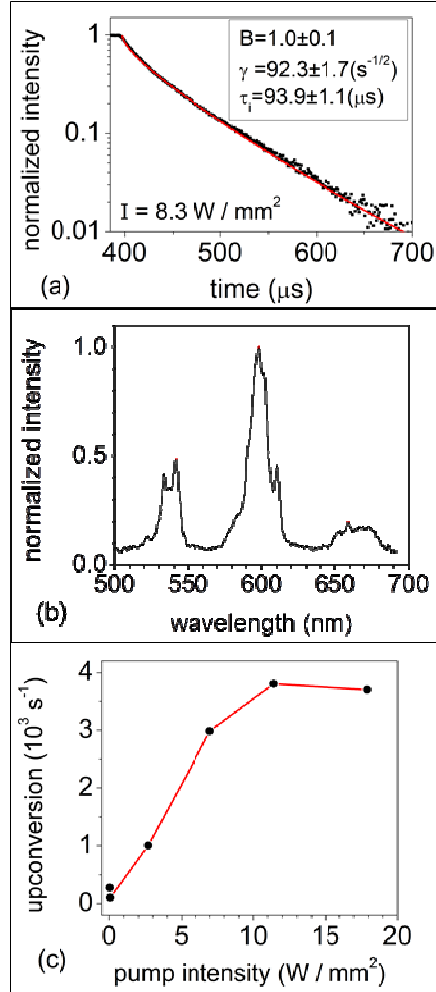


Fig. 10. (a) ${}^4F_{3/2} \rightarrow {}^4I_{11/2}$ spontaneous transition decay and fit with Eq. (3) for a pump intensity of 8.3 W/mm^2 (b) spectra of up-conversion emissions. (c) Saturation of the up-conversion rate as a function of the pump intensity.

The ETU rate $W_{UP} (\text{s}^{-1})$ shown in Fig. 10(c) is obtained using the following Eq.:

$$W_{UP} (\text{s}^{-1}) = 1/\tau_{\text{int}} - 1/\tau_i \quad (4)$$

where τ_{int} is the integration decay time. Because τ_{int} is dependent on the pump intensity (I), the evolution of the ETU rate $W_{UP} (\text{s}^{-1})$ can be obtained by measuring τ_{int} for different pump intensities $I (\text{W/mm}^2)$. From this analysis it is possible to determine the dependence of the

upconversion rate W_{UP} on the pump intensity, which is particularly interesting as it is a mechanism that introduces a loss channel for devices emitting in the infrared region [17].

4. Conclusion

In summary, we have studied for the first time random laser action in nano powders of $Nd^{3+}:YVO_4$. We show stimulated emission at the ${}^4F_{3/2} \rightarrow {}^4I_{11/2}$ transition (1064 nm). Other emissions suffer spectral quenching. An alternative method to characterize the emission dynamics for long pump pulses has been developed without the necessity of observation of relaxations oscillations. By this analysis it is possible to determine the fraction of the stimulated and spontaneous contribution in the emission. It was shown that the slow laser line narrowing of the random laser is due to a rather slow increase in stimulated emission while a considerable fraction of spontaneous emission remains present in the backscattering cone for all tested pump intensities.

We also presented a method to determine the ETU transfer rate (and its saturation rate) through the Inokuti-Hirayama model for this strongly scattering media.

Acknowledgments

The authors thank the Support from Fundação de Amparo à Pesquisa do Estado de São Paulo (FAPESP), Conselho Nacional de Desenvolvimento Científico e Tecnológico (CNPq) and Instituto Nacional de Ciência e Tecnologia (INCT).